Strong-Field Spatial Interference in a Tailored Electromagnetic Bath

Mihai Macovei,[1] Jörg Evers,[1] Gao-xiang Li,[2,1] and Christoph H. Keitel[1]

[1]*Max-Planck-Institut für Kernphysik, Saupfercheckweg 1, D-69117 Heidelberg, Germany*

[2]*Department of Physics, Huazhong Normal University, Wuhan 430079, China*

(Received 9 June 2006; published 24 January 2007)

Light scattered by a regular structure of atoms can exhibit interference signatures, similar to the classical double-slit. These first-order interferences, however, vanish for strong light intensities, restricting potential applications. Here, we show how to overcome these limitations to quantum interference in strong fields. First, we recover the first-order interference in strong fields via a tailored electromagnetic bath with a suitable frequency dependence. At strong driving, the optical properties for different spectral bands are distinct, thus extending the set of observables. We further show that for a two-photon detector as, e.g., in lithography, increasing the field intensity leads to twice the spatial resolution of the second-order interference pattern compared to the weak-field case.

DOI: 10.1103/PhysRevLett.98.043602 PACS numbers: 42.50.Hz, 42.50.Ct, 42.50.St

If light is scattered by a structure such that different indistinguishable pathways connect source and detector, then interference effects may arise [1]. The classical example is the double-slit experiment, demonstrated experimentally in numerous different setups [2]. A modern archetype realization employs two nearby atoms scattering near-resonant laser light [3–7]. As compared to single-atom systems, the geometry of the two-particle setup gives rise to interference phenomena in the scattered light. In particular, the beautiful experiment by Eichmann *et al.* [3] has led to a discussion on the interpretation of the first-order interference effects in terms of a double slit [5]. This interference, however, is restricted to low incident light intensity and vanishes at strong driving [5–9]. The reason is that in the strong-field limit, the two-particle collective dressed states are uniformly populated, such that the interference fringe visibility is zero. This restricts potential applications, as has been repeatedly reported in different areas of optical physics. For example, coherent backscattering from disordered structures of atoms predominantly relies on the interference of coherently scattered light [8], as well as the generation of squeezed coherent light by scattering light off of a regular structure [9]. Other applications are lithography [10], where writing structures with high contrast requires a large visibility, or precision measurements and optical information processing, where strong light fields may lead to increased resolution, high signal-to-noise ratios or a rapid coherent system evolution. More generally, the strong-field limit is desirable, as then the different lines of the spectrum are well separated, just as in the Mollow resonance fluorescence spectrum of a single strongly driven two-level atom. The spectral separation allows for a clearer interpretation and gives rise to an extended set of observables.

Thus, in this Letter, we discuss quantum interference in strong driving fields. First, we demonstrate how to recover the first-order interference fringes in the strong-field case. This is achieved by mediating the atom-laser interactions through a surrounding bath with different photon mode densities at the various dressed-state frequencies. Techniques to modify the vacuum as required here have been demonstrated in various contexts [11,12]. The spontaneous decay rates are proportional to the density of modes at the transition frequencies, and thus the dressed-state populations redistribute. As in the strong-field limit the spectral lines are well separated, we are led to define optical properties for each of the spectral lines separately, yielding an extended set of observables. We show that by a suitable redistribution of the dressed-state populations, full interference fringe visibility can be achieved in the central band of the emitted light, thus demonstrating the recovery of the interference. Interestingly, in this case, the scattered light is entirely coherent despite the strong driving. Second, we investigate the spatial dependence of the second-order correlation function and focus on the case of a single two-photon detector, as, for example, in lithography with a medium sensitive to two-photon exposure. We show that in this setup, by increasing the driving field intensity, the spatial resolution of the central strong-field second-order interference pattern can be increased by a factor of 2 as compared to the corresponding weak-field pattern. Thus structures with high spatial resolution and signal intensity can be created using strong driving fields. Our scheme can be realized in a wide range of systems, and can also be reversed to analyze the structure of the scatterers, as discussed later. Finally, we generalize our results to the case of a linear chain of N atoms.

The model.—We first investigate a pair of distinguishable nonoverlapping two-state emitters, a and b, both with atomic transition frequency ω_0, at positions $\vec{r}_a$, $\vec{r}_b$, and separated by $\vec{r}_{ab}$. The external laser field has frequency $\omega_L = ck_L$, wave vector $\vec{k}_L$, and is aligned such that $\vec{k}_L \cdot \vec{r}_{ab} = 0$ (see Fig. 1). Our aim is to induce interference phenomena in the light scattered by these radiators in the intense driving field limit. We treat the problem in a general form, comprising any form of the environmental electromagnetic field (EMF) satisfying the Born-Markov conditions. The results will be generalized to a linear

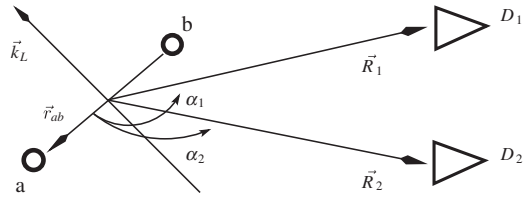

FIG. 1. Two nearby two-state emitters a and b, separated by $\vec{r}_{ab}$, and driven by a resonant strong external laser field with wave vector $\vec{k}_L$. Detectors $\{D_1, D_2\}$ are used to measure correlations among the emitted photons. $\{\alpha_1, \alpha_2\}$ are the angles between $\vec{r}_{ab}$ and the observation directions $\{\vec{R}_1, \vec{R}_2\}$.

structure of $N > 2$ atoms in the final part. The laser-dressed atomic system is described, in the electric dipole and rotating wave approximations, by the Hamiltonian $H = H_0 + H_I$, where

$$H_0 = \sum_k \hbar(\omega_k - \omega_L) a_k^\dagger a_k + \sum_{j\in\{a,b\}} \hbar\tilde{\Omega}_j R_{zj}, \tag{1}$$

$$H_I = i\sum_k \sum_{j\in\{a,b\}} (\vec{g}_k \cdot \vec{d}_j)\Big\{a_k^\dagger\Big(R_{zj}\frac{\sin 2\theta_j}{2} - R_{21}^{(j)}\sin^2\theta_j + R_{12}^{(j)}\cos^2\theta_j\Big)e^{-i(\vec{k}-\vec{k}_L)\cdot\vec{r}_j} - \text{H.c.}\Big\}. \tag{2}$$

H_0 represents the Hamiltonian of the free EMF and free dressed atomic subsystems, respectively, while H_I accounts for the interaction of the laser-dressed atoms with the EMF. a_k and $a_k^\dagger$ are the radiation field annihilation and creation operators obeying the commutation relations $[a_k, a_{k'}^\dagger] = \delta_{kk'}$, and $[a_k, a_{k'}] = [a_k^\dagger, a_{k'}^\dagger] = 0$. The atomic operators $R_{\alpha\beta}^{(j)} = |\tilde{\alpha}\rangle_{jj}\langle\tilde{\beta}|$ describe the transitions between the dressed states $|\tilde{\beta}\rangle_j$ and $|\tilde{\alpha}\rangle_j$ in atom j for $\alpha \neq \beta$ and dressed-state populations for $\alpha = \beta$, and satisfy the commutation relation $[R_{\alpha\beta}^{(j)}, R_{\alpha'\beta'}^{(l)}] = \delta_{jl}[\delta_{\beta\alpha'}R_{\alpha\beta'}^{(j)} - \delta_{\beta'\alpha}R_{\alpha'\beta}^{(j)}]$. The operators $R_{\alpha\beta}^{(j)}$ can be represented through the bare state operators via the transformations $|1\rangle_j = \sin\theta|\tilde{2}\rangle_j + \cos\theta|\tilde{1}\rangle_j$ and $|2\rangle_j = \cos\theta|\tilde{2}\rangle_j - \sin\theta|\tilde{1}\rangle_j$. We define $R_{zj} = |\tilde{2}\rangle_{jj}\langle\tilde{2}| - |\tilde{1}\rangle_{jj}\langle\tilde{1}|$. Further, $\tilde{\Omega} = \tilde{\Omega}_j = [\Omega^2 + (\Delta/2)^2]^{1/2}$ is the generalized Rabi frequency, with $2\Omega = (\vec{d}\cdot\vec{E}_L)/\hbar$. Here, E_L is the electric laser field strength, and $\vec{d} \equiv \vec{d}_a = \vec{d}_b$ is the transition dipole matrix element. The detuning $\Delta = \omega_0 - \omega_L$ is characterized by $\cot 2\theta = \Delta/(2\Omega)$. The dressed-state transition frequencies are ω_L, $\omega_\pm = \omega_L \pm 2\tilde{\Omega}$.

The two-particle spontaneous decay and the vacuum-mediated collective interactions are given by the frequency-dependent expression

$$\gamma_{jl}(\omega) = \hbar^{-2}\sum_k (\vec{g}_k \cdot \vec{d})^2 e^{i\vec{k}\cdot\vec{r}_{jl}}\Theta(\omega_k, \omega) = \gamma(\omega)[\chi_{jl}(\omega) + i\Omega_{jl}(\omega)]. \tag{3}$$

The coupling constant between atom and environment is g_k, while $\Theta(\omega_k, \omega)$ defines the structure of the Markovian bath. Independent of the atom-vacuum coupling, the collective parameters χ_{jl} and Ω_{jl} $(j \neq l)$ tend to zero in the large-distance case $r_{jl} \to \infty$ which corresponds to the absence of coupling among the emitters.

Intensities.—Driving a single two-state atom with a strong near-resonant laser field splits the resonance fluorescence spectrum into the well-known three-peaked Mollow spectrum. Then it is reasonable to consider optical properties for each spectral band separately. A similar splitting occurs in a two-atom system. If the laser beam is perpendicular to the line connecting the atoms, i.e., $\vec{k}_L \cdot \vec{r}_{ab} = 0$, then the central (CB) and left or right sideband (LB or RB) spectral intensities are given by

$$I_{\text{CB}}(\vec{R}_1) = \frac{1}{4}\sum_{j,l\in\{a,b\}} \Psi_{R_1}(\vec{r}_{jl}, \omega_L)\langle R_{zj}R_{zl}\rangle \sin^2 2\theta, \tag{4a}$$

$$I_{\text{LB}}(\vec{R}_1) = \sum_{j,l\in\{a,b\}} \Psi_{R_1}(\vec{r}_{jl}, \omega_-)\langle R_{12}^{(j)}R_{21}^{(l)}\rangle \sin^4\theta, \tag{4b}$$

$$I_{\text{RB}}(\vec{R}_1) = \sum_{j,l\in\{a,b\}} \Psi_{R_1}(\vec{r}_{jl}, \omega_+)\langle R_{21}^{(j)}R_{12}^{(l)}\rangle \cos^4\theta. \tag{4c}$$

Here, $\Psi_{R_1}(\vec{r}_{jl}, \omega) = \Psi_{R_1}(\omega)\exp[i(\omega/c)r_{jl}\cos\alpha_1]$ with angle α_1 between observation direction $\vec{R}_1$ and distance vector $\vec{r}_{jl}$. This prefactor depends on the atom-environment coupling and in general the frequency with $R_1 = |\vec{R}_1| \gg k_L^{-1}$. We have assumed the strong-field limit $\tilde{\Omega} \gg \{\gamma(\omega_+), \gamma(\omega_-), \gamma(\omega_L)\}$ and $\tilde{\Omega} \gg \{\gamma(\omega_+)\Omega_{ab}(\omega_+), \gamma(\omega_-)\Omega_{ab}(\omega_-), \gamma(\omega_L)\Omega_{ab}(\omega_L)\}$ in deriving Eqs. (4). Note that multiatom systems may exhibit additional spectral line splittings due to the dipole-dipole interaction between the emitters, if the interatomic distance is small compared to the transition wavelength.

Visibilities.—If the interparticle separation is large enough to ignore the line splittings caused by dipole-dipole interactions, then the visibilities $V = [I_{\max} - I_{\min}]/[I_{\max} + I_{\min}]$ for each of the central, left, and right spectral band follow from Eqs. (4) as

$$V_{\text{CB}} = \sigma_{ee} + \sigma_{gg} - \sigma_{ss} - \sigma_{aa}, \tag{5a}$$

$$V_{\text{LB(RB)}} = [\sigma_{ss} - \sigma_{aa}]/[1 \mp \sigma_{ee} \pm \sigma_{gg}]. \tag{5b}$$

We have introduced in Eq. (5) the two-atom collective dressed states as $|\Psi_e\rangle = |\tilde{2}_a, \tilde{2}_b\rangle$, $|\Psi_{s(a)}\rangle = \{|\tilde{2}_a, \tilde{1}_b\rangle \pm |\tilde{2}_b, \tilde{1}_a\rangle\}/\sqrt{2}$, $|\Psi_g\rangle = |\tilde{1}_a, \tilde{1}_b\rangle$. The expectation values $\sigma_{\alpha\beta} = \langle|\Psi_\alpha\rangle\langle\Psi_\beta|\rangle$ describe the corresponding transitions $(\alpha \neq \beta)$ and populations $(\alpha = \beta)$ $(\{\alpha, \beta\} \in \{e, s, a, g\})$. If the population is now transferred into a particular collective dressed state, then the spectral band visibilities will behave according to Eqs. (5). One can easily observe that all visibilities vanish if the atomic population is uniformly distributed over two-particle collective dressed states, recovering previous results [5–7].

Two-particle quantum dynamics.—Introducing the notations $x = 2(\sigma_{ee} - \sigma_{gg})$, $y = \sigma_{ss} - \sigma_{aa}$, and $z = \sigma_{ee} + \sigma_{gg} - \sigma_{ss} - \sigma_{aa} \equiv V_{\mathrm{CB}}$, the dressed-state atomic correlators in Eqs. (4) and (5) follow from Eqs. (1) and (2) as [13]

$$\dot{x}(t) = -2\xi^{(+)}x + 4\zeta_{ab}^{(-)}y + 4\xi^{(-)}, \tag{6a}$$

$$\dot{y}(t) = -\zeta_{ab}^{(-)}x - 2(c_{ab}^{(0)} + \xi^{(+)})y + 2\zeta_{ab}^{(+)}z, \tag{6b}$$

$$\dot{z}(t) = 2\xi^{(-)}x + 4\zeta_{ab}^{(+)}y - 4\xi^{(+)}z. \tag{6c}$$

The coefficients are $\xi^{(\pm)} = \gamma(\omega_-)\sin^4\theta \pm \gamma(\omega_+)\cos^4\theta$, $\zeta_{ab}^{(\pm)} = \gamma(\omega_-)\chi_{ab}(\omega_-)\sin^4\theta \pm \gamma(\omega_+)\chi_{ab}(\omega_+)\cos^4\theta$, and $c_{ab}^{(0)} = \gamma(\omega_L)[1 - \chi_{ab}(\omega_L)]\sin^2 2\theta$. Simple analytical expressions for the two-atom steady-state quantum dynamics can be obtained in some particular cases. For example, for the large-distance case $k_L r_{ab} \gg 2\pi$ one obtains $\zeta_{ab}^{(\pm)} \to 0$ and $c_{ab}^{(0)} \to \gamma(\omega_L)\sin^2 2\theta$, such that

$$x = 2\xi^{(-)}/\xi^{(+)}, \qquad y = 0, \quad \text{and} \quad z = [\xi^{(-)}/\xi^{(+)}]^2. \tag{7}$$

In this case, the diagonal atomic dynamics is independent of the interatomic separation.

First-order interference pattern.—For resonant driving ($\theta = \pi/4$), the atomic population is equally distributed over the two-atom dressed states resulting in the absence of an interference pattern. Only small values for V_{CB} can be obtained for off-resonant pumping, while V_{LB} and V_{RB} are always zero [see Eqs. (5) and (7)]. A weak interference pattern can be induced in the sidebands if the splitting of the dressed levels is large such that $2\tilde{\Omega}/\omega_0 \ll 1$ is not negligible. Then the dressed states couple differently to the EMF, i.e., $\gamma(\omega_-)\chi_{ab}(\omega_-) \neq \gamma(\omega_+)\chi_{ab}(\omega_+) \neq 0$ [13]. Nevertheless, for practical situations, the first-order interference vanishes for a strongly driven atomic pair in free space.

In the following, we show how the interference can be recovered for two strongly driven atoms by modifying the surrounding electromagnetic reservoir. In effect, this alters the parameter $\eta = \gamma(\omega_+)/\gamma(\omega_-)$, which in free space is 1. We assume the driving fields to be on resonance, i.e., $\theta = \pi/4$, with $\Omega \gg \{\gamma(\omega_\pm), \gamma(\omega_L)\}$. Figure 2 shows the dependence of the central spectral band visibility, $V_{\mathrm{CB}} = [(1 - \eta)/(1 + \eta)]^2$, versus the ratio η. Maximum visibility ($V_{\mathrm{CB}} = 1$) can be obtained for $\eta \ll 1$ or $\eta \gg 1$. This corresponds to an interference pattern with a bright center. In these cases, $\sigma_{ee} \to 1$ ($\eta \ll 1$) or $\sigma_{gg} \to 1$ ($\eta \gg 1$), while the other two collective dressed states are empty ($\sigma_{ss} = \sigma_{aa} = 0$). Thus, $V_{\mathrm{LB}} = V_{\mathrm{RB}} = 0$. In other words, if the densities of the EMF modes at the dressed transition frequencies $\omega_\pm = \omega_L \pm 2\tilde{\Omega}$ differ considerably, then $\eta \ll 1$ or $\eta \gg 1$, and the interference pattern is recovered in the central band. Figure 3 shows a corresponding interference pattern versus detection angle α. We now analyze the interference in terms of scattering via symmetric and antisymmetric collective states [6]. Transitions involving symmetric [antisymmetric] collective states give rise to interference with a bright [dark] center. If both channels have equal probability, the interference fringes wash out. In our system for $\eta \ll 1$ or $\eta \gg 1$, however, only symmetric collective states are populated, as can be seen from the definition of $|\Psi_e\rangle$ and $|\Psi_g\rangle$. Thus we always find bright center interference. Note that independent of the collective state, the single-atom dressed states can be either symmetric ($|\tilde{2}\rangle$) or antisymmetric ($|\tilde{1}\rangle$).

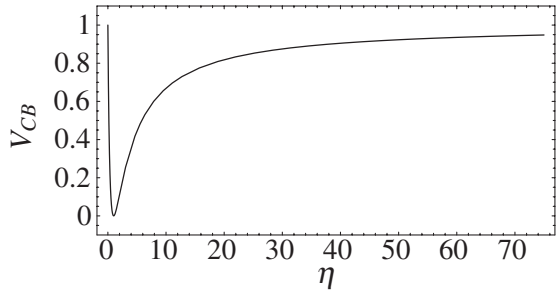

FIG. 2. Central-band visibility V_{CB} as a function of η for $\theta = \pi/4$ and $k_L r_{ab} \gg 2\pi$.

Our scheme can, for example, be implemented by trapping the scatterers in a cavity with suitable frequency dependence. Experiments on modifying the single-atom Mollow spectrum in cavities have already been reported [11]. Other methods are to embed the two particles in a photonic band-gap material [12], or to additionally pump the dressed-atom sample with chaotic fields [14]. The experimental control of population in an artificial two-state atom [15] suggests a possible realization in mesoscopic systems. Our results can also be used to analyze the structure of the scattering material, e.g., the geometric distribution of the scatterer, in particular, using the extension to many scatterers discussed below.

Second-order correlation functions.—We now turn to the second-order correlation function of the resonance fluorescence emitted in the three spectral bands,

$$g_{\mathrm{CB}}^{(2)}(\vec{R}_1, \vec{R}_2) = 1 + \frac{(1 - V_{\mathrm{CB}}^2)\cos\delta_1^{(0)}\cos\delta_2^{(0)}}{D_{\mathrm{CB}}}, \tag{8a}$$

$$g_{\mathrm{LB,RB}}^{(2)}(\vec{R}_1, \vec{R}_2) = \frac{p_{L,R}[1 + \cos(\delta_1^{(\mp)} - \delta_2^{(\mp)})]}{D_{\mathrm{LB,RB}}}. \tag{8b}$$

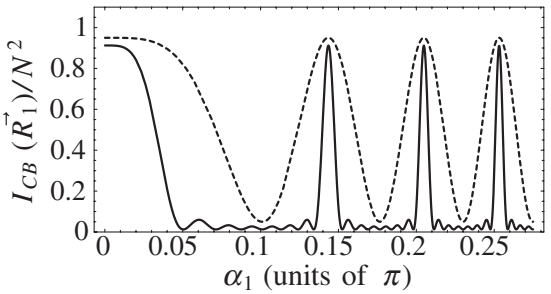

FIG. 3. Central-band intensity $I_{\mathrm{CB}}(\vec{R}_1)/N^2$ [in units of $\Psi_{R_1}(\omega_L)/4$] as a function of α_1. Here $\theta = \pi/4$, $k_L r_{ab} = 20\pi$ and $V_{\mathrm{CB}} = 0.9$. Solid line: $N = 8$, dashed curve: $N = 2$.

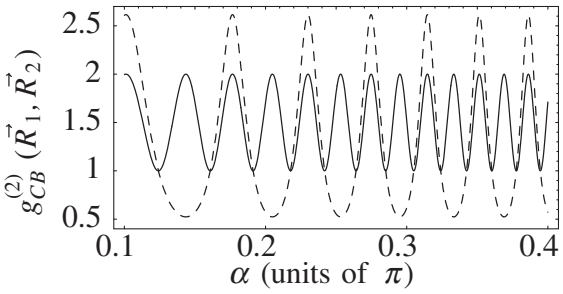

FIG. 4. Central-band second-order correlation function $g^{(2)}_{\mathrm{CB}}(\vec{R}_1, \vec{R}_2)$. The solid line depicts the strong-field limit ($V_{\mathrm{CB}} = 0$) while the dashed curve describes the weak-field case with $\Omega/\gamma = 0.9$. Here $\Delta = 0$, $k_L r_{ab} = 20\pi$, and $\vec{R}_1 = \vec{R}_2$.

Here, $D_n = \prod_{m\in\{1,2\}}[1 + V_n \cos\delta_m^{(n)}]$, and $p_L = 2\sigma_{gg}/[1 - \sigma_{ee} + \sigma_{gg}]^2$, and $p_R = 2\sigma_{ee}/[1 + \sigma_{ee} - \sigma_{gg}]^2$. The argument $\delta_m^{(n)} = k_n r_{ab} \cos\alpha_m$ ($m \in \{1, 2\}$) is evaluated at frequency $\{\omega_L, \omega_-, \omega_+\}$ with wavevector k_n for the respective n values $\{0 = \mathrm{CB}, - = \mathrm{LB}, + = \mathrm{RB}\}$.

For $V_{\mathrm{CB}} = 1$, one finds $g^{(2)}_{\mathrm{CB}}(\vec{R}_1, \vec{R}_2) = 1$, i.e., fully coherent light. In the absence of first-order interference ($V_{\mathrm{CB,LB,RB}} = 0$), in the standard vacuum, the second-order correlation functions do exhibit interference:

$$g^{(2)}_{\mathrm{CB}}(\vec{R}_1, \vec{R}_2) = 1 + \cos\delta_1 \cos\delta_2, \tag{9a}$$

$$g^{(2)}_{\mathrm{LB,RB}}(\vec{R}_1, \vec{R}_2) = [1 + \cos(\delta_1 - \delta_2)]/2. \tag{9b}$$

Our main interest here is the second-order spatial interference resolution [10] for a two-photon detector with $\delta_1 = \delta_2 \equiv \delta$, e.g., a medium sensitive to two-photon exposure. In the strong-field limit $\Omega/\gamma \gg 1$, from Eq. (9) we find $g^{(2)}_{\mathrm{CB}}(\vec{R}) = 1 + \cos^2\delta$. In the weak-field case $\Omega/\gamma < 1$ without spectral band separation, however, one finds $g^{(2)}(\vec{R}) = [s/(s + \cos\delta)]^2$ with $s = 1 + 2(\Omega/\gamma)^2$ [6]. Remarkably, increasing the driving field strength effectively doubles the spatial fringe resolution in the central spectral band in this detector setup relevant, e.g., to lithography. This is illustrated in Fig. 4, which shows both cases as function of the detector positions. Thus high-resolution spatial structures can be achieved using strong driving fields. We note in passing that sub-Poissonian or Poissonian photon statistics [16] can be generated in all three spectral lines, and super-Poissonian photon statistics in the central band, see, e.g., Eq. (9).

Multiatom sample.—We now extend our first-order interference analysis to a many-atom ensemble. If N independent two-level emitters are uniformly distributed in a linear chain ($r_{ab} = r_{i,i-1}$), then their central-band intensity [in units of $\sin^2(2\theta)\Psi_R(\omega_L)/4$] evaluates to

$$I_{\mathrm{CB}}(\vec{R}_1) = N(1 - z) + z\mathcal{F}(\delta_1). \tag{10}$$

Here, $\delta_i = k_L r_{ab} \cos\alpha_i$, $\mathcal{F}(x) = \sin^2[Nx/2]/\sin^2[x/2]$, and z is given in Eq. (7). Maxima of I_{CB} occur for $k_L r_{ab} \cos\alpha = 2\pi n$ with $z = 1$, where $I^{(\mathrm{max})}_{\mathrm{CB}}(\vec{R}) \propto N^2$. Thus the central-band visibility is significantly improved (see Fig. 3), while the subwavelength pattern resolution scales with the atom number [1].

In summary, it was shown how first-order interference can be recovered in the fluorescence light of strongly driven atoms. The key idea is to modify the surrounding electromagnetic vacuum, giving rise to a redistribution of the collective dressed-state populations. Under strong driving, visibilities have to be defined for each emitted spectral band separately, providing an extended set of observables. Finally, the second-order interference fringes for two-photon detection have double resolution in the strong-field case as compared to the weak-field pattern.

[1] M. Born and E. Wolf, *Principles of Optics* (Cambridge University Press, Cambridge, England, 1999).
[2] F. Lindner *et al.*, Phys. Rev. Lett. **95**, 040401 (2005), and references therein; M. Kiffner, J. Evers, and C. H. Keitel, Phys. Rev. Lett. **96**, 100403 (2006).
[3] U. Eichmann *et al.*, Phys. Rev. Lett. **70**, 2359 (1993).
[4] J. Eschner *et al.*, Nature (London) **413**, 495 (2001).
[5] T. Richter, Opt. Commun. **80**, 285 (1991); P. Kochan *et al.*, Phys. Rev. Lett. **75**, 45 (1995); G. M. Meyer and G. Yeoman, *ibid.* **79**, 2650 (1997); T. Wong *et al.*, Phys. Rev. A **55**, 1288 (1997); W. H. Itano *et al.*, *ibid.* **57**, 4176 (1998); T. Rudolph and Z. Ficek, *ibid.* **58**, 748 (1998); G. Yeoman, *ibid.* **58**, 764 (1998); Ch. Schön and Almut Beige, *ibid.* **64**, 023806 (2001).
[6] C. Skornia *et al.*, Phys. Rev. A **64**, 063801 (2001).
[7] G. S. Agarwal *et al.*, Phys. Rev. A **65**, 053826 (2002).
[8] V. Shatokhin *et al.*, Phys. Rev. Lett. **94**, 043603 (2005).
[9] W. Vogel and D.-G. Welsch, Phys. Rev. Lett. **54**, 1802 (1985).
[10] A. N. Boto *et al.*, Phys. Rev. Lett. **85**, 2733 (2000); M. D'Angelo, M. V. Chekhova, and Y. Shih, *ibid.* **87**, 013602 (2001); J. Xiong *et al.*, *ibid.* **94**, 173601 (2005); P. R. Hemmer *et al.*, *ibid.* **96**, 163603 (2006); C. H. Keitel and S. X. Hu, Appl. Phys. Lett. **80**, 541 (2002).
[11] Y. Zhu *et al.*, Phys. Rev. Lett. **61**, 1946 (1988); A. Lezama *et al.*, Phys. Rev. A **39**, R2754 (1989).
[12] M. Florescu and S. John, Phys. Rev. A **69**, 053810 (2004).
[13] M. Dal Col, M. Macovei, and C. H. Keitel, Opt. Commun. **264**, 407 (2006).
[14] G.-x. Li, J. Peng, and G. Huang, J. Phys. B **33**, 3743 (2000).
[15] J. R. Petta *et al.*, Phys. Rev. Lett. **93**, 186802 (2004).
[16] D. F. Walls and G. S. Milburn, *Quantum Optics* (Springer, Berlin, 1994).